ESTIMATION OF FRACTURE TOUGHNESS FOR A PIPE MATERIAL USED FOR NATURAL GAS TRANSPORT

H. Drar & Y.F. Al-Obaid

Faculty of Technological Studies, [PAAET], Kuwait.

ABSTRACT:

This paper discusses the problem of determining the characteristic values in ductile fracture mechanics on the basis of the fracture toughness, K_{Ic}, for a double-sided spiral submerged arc weld pipeline material. Special interest was directed towards using the material from the relatively thin ready-to-use pipe of the hot rolled steel API 5L-X52. For this purpose Charpy V-notch impact test on subsized specimens were performed at temperature ranging from -80 to 0°C. The specimens were taken from the weld zone and the parent material remote from the welds. The V-notch were so oriented as to reproduce the fracture path which would result through the pipe-thickness.

Using the estimated K_{Ic} from the above measurements and the available design-data for the pipeline, the maximum acceptable sizes of different defects were calcualted. The variability of material properties and stresses about the assumed design values were also treated statistically to ensure that the standard for detection of a tolerable defect size at a required probability can be established.

KEYWORDS: Pipeline failure, Ferritic steel, Weldment, Tensile properties, Charpy energy, Fracture mechanics, Toughness.

INTRODUCTION

The work reported upon here was motivated by the desire to provide

information about the allowable flaw sizes in submerged arc welded pipe. The pipe is intended for natural gas transmission pipelines: outer diameter ca 406 mm (16"), wall thickness 6.35 mm (0.25") and of a hot rolled steel according to API 5L-X52. The maximum allowable internal pressure at unsteady flow conditons of the pipeline is ca 7 MPa (1000 psi).

The accelerated thinning at specific locations of a pipeline can hardly be avoided. An example is a low dip in a condensate line. In such a case this dip in the line is the most likely place for water to accummulate causing internal corrosion process of the pipe line to develop at a fast rate. The internal protection at such locations, e.g. coating with coal tar epoxy, can slow down the thinning rate of the pipe wall but does not eliminate the process.

The present investigation was limited to study the local thinly pipe-wall levels at which failure is most likely to occure under well defined operating conditions. No attempt was undertaken to attack the corrosion problem or the growth mechanisms of the defects either these are inherently present or introduced during construction or service. Thus the interested type of flaw which can be postulated in our case is a surface crack on the inside surface of the pipe.

The critical flaw sizes were calculated using two distinct fracture-mechanics analysis methods [1,2] and the maximum operating stresses from the internal gas pressure and the necessary material properties. In this analysis the flaws were taken axially aligned and therefore the hoop stress corresponding to the nominal line pressure was considered.

An attempt has been tried to make analysis of two distinct regions of the pipe; at the weld seam and at the base metal. At each region we integrate the possible effect of the rolling direction to the analysis.

Finally the results of our study were compared with the available actual thickness readings at fracture faces of a similar pipe ruptured from a pipe

line of comparable working conditions.

EXPERIMENTAL WORK

The material tested is a full killed hot rolled steel with the chemical composition shown in table 1. The carbon equivalent was estimated as 0.27%. The tensile mechanical properties were certified from the supplier as yield strength: σ = 460 MN/m^2 and ultimate tensile strength: σ_u = 560 MN/m and elongation of 32% at 50 mm gauge length.

Fig.1 summarizes the relative positions of the four-specimen-types considered for measuring the tensile properties of the pipe. The shown plates were oxygen-cutted from the delivered pipe segment (6 m long), and a hydraulic press was used for flattening the plates. The effect of oxygen flame was then removed by saw-cutting the periphery of the flattened plates to strip-sheets of ca 300 x 40 mm. These flat specimens were then machined ca 1 mm from each side to remove the effect of plastic deformation due to the pressing operation, resulting in specimens of ca. 4 mm thickness. Some of the above "raw" specimens, i.e. the flat sheet of 300 x 35 x 4 mm, were machined to the recommended shape given in fig.3 of the BS 709: 1983. The original cross section area of these specimens is approx. 20 x 4 mm.

Some of the specimens were also machined to produce strip of only the weld plus HAZ in the tensile direction. The original area of such specimens were 10 x 4 mm.

The Charpy Vee Notch (CVN) specimens were fabricated from the pipe material without flattening. Two series of CVN specimens were machined from the pipe material, fig. 2. In both series the notch is placed in the thickness direction of the pipe. The resulted subsize specimens, were of ca 5 mm thickness.

Tensile tests were run in an Instron machine where the load versus displacement, measured from the position of the moving 5 mm/min cross-head, could be recorded continuously. Charpy test was conducted in an AVERY machine

while the value of the specimen temperature, initially decreased by liquid nitrogen, could be followed by a digital thermometer. The major constitutents of the microstructures has been found to be ferrite and less than 5 vol % pearlite with average hardness of 130 HV30.

RESULTS AND ANALYSIS

Figure 3 shows the results of the tensile tests of the four specimen-types. Each curve is the average of three tests of the same specimen. The individual values of σ_y and σ_u are given in fig.4. As it can be seen from fig.1, the specimens types 1 and 4 are taken in rolling direction while 2 and 3 are perpendicular to the rolling direction.

Two degrees of confidence, 67 and 99%, in the σ_y - mean of the three tests were calculated by the statistical method of t-distribution, [3], the results are seen in fig.5.

The effect of integrating the weld and HAZ to the base metal was further emphasized by the results of tensile testing the weld + HAZ alone. Table 2 shows the results taken from testing three small specimens of type 1 and 4.

The results of CVN are shown in Fig.6. The fracture energy of each specimen was normalized by the area under the notch. The average area of the 27 specimens from the base metal was 43.48 mm^2 with standard deviation $\pm$ 2.48 mm^2 . For the 11 specimens taken from the weld metal and HAZ the corresponding area was 42.24 mm^2 and 1.15 mm^2.

The fracture energy at each temperature, 3 values, were statistically treated, using the t-distribution method,to calculate the standard deviation of the mean and the degree of confidence. The degree of confidence that the shown mean actually lies between the shown limits in fig. 7 is 95%.

FRACTURE TOUGHNESS

For our thin ferritic pipe material, K_{Ic} was evaluated using the method described in the BS PD 6493. The mean values of CVN for base metal and for the weld + HAZ at 0 ^{o}C (162 and 62 J/cm^2 respectively) were used with Figs.20a

and 20b to find pessimistic values of K_{Ic}. The assumed operating temperature here was 10°C and the resulted minimum values of K_{Ic} were 123 and 55 MP $\sqrt{m}$ for the base and weld metal respectively.

The relationship between Charpy shelf energy and K_c was demonstrated for pipeline materials by Maxey et al [4]. This was done by comparing the strain energy release rate calculated from full-scale test results, with the ductile shelf energy for 2/3 standard size specimens per unit area of CVN - bars of the material, and the following relation was suggested:

$$C_v/A = K_c^2 / E \quad \ldots \quad (1)$$

where C_v is the measured shelf energy , A is the area of fracture surface of the CVN-specimen and E is the modulus of elasticity.

The choosen C_v was taken as it is found in [1] for the pipe of the nearest dimension to ours and of the same API grade, i.e.X-52. The value of C_v in this case is 25.7 J and it was measured for 16" diameter pipe with wall thickness of 0.290" (cf. 16" and 0.250" for our pipe).

The value of E given by the steel supplier was 192 GPa. From literature we were convinced that E for similar pipe material was not far from this value but even larger, e.g. E = 208 GPa for API 5LX-65 in,[5].

Using the above value of C_v with E = 192 GPa and A as 2/3 the standard size of Charpy area under the notch in eqn.1 gave K_c = 300 MPa$\sqrt{m}$.

CRITICAL FLAW SIZE.

Critical flaw sizes of our pipe at the given working conditions were evaluated by two methods.

Kiefner's Model

The model applies to axial flaw, as of interest in our case, and was developed on the basis of full-scale pipe rupture tests. Thus the model is basically a semi-empirical, and Kiefner found that plastic instability leading to rupture occurs when the applied stress on the pipe due to the internal pressure reaches a critical value, failure stress σ_c, related to

surface flaw size (length 2c, depth d), material flow strength ($\bar{\sigma}$) and the pipe dimensions (radius R, thickness t).

$$\sigma_c = \bar{\sigma} \cdot f(d,c,R,t) \quad \ldots \quad (2)$$

The function f(d,c,R,t) was able to predict the failure stress σ_c , for surface flaws successfully when: $0.3 \leqslant d/t \leqslant 0.7$. Since we were interested in the axial flaw sizes (2c,d) at which plastic instability started under normal working conditions, then the failure stress of eqn.2 was taken equal to the hoop stress which results from the internal pressure of the transmitted gases, P. The hoop stress in the pipe wall was approximated by using the simple thin walled pressure vessel theory: $\sigma_h = PR/t = 220$ MPa. In fact, the final stage of failure in pipes of similar working conditions, have shown that surface flaws extend with increasing load primarily in the through-the-thickness direction, [6]. Thus choosing the circumference stress is well motivated.

The value of flow stress for pipeline material can be taken as,[2,6]:

$$\sigma = \sigma_y \text{ (Ksi)} + 10 \text{ (Ksi)} \quad \ldots \quad (3)$$

$$\sigma = (\sigma_y + \sigma_u)/2 \quad \ldots \quad (4)$$

The two equations gave values around 500 MPa, $\sigma_y \simeq$ 430 MPa and $\sigma_u \simeq$ 565 MPa,and therefore this value will be used in our calculations. The classic model of Kiefner suggests two different functions f_1 and f_2 depending on the pipe-failure-mode. Fig. 8 illustrates the two different failure modes, their relation to the failure stress and the flaw size. The flaw sizes in section A, represent the failure mode which is independent of the flaw sizes. The pipe containing such flaw sizes will be said its material is flow stress dependent. The material flow stress, $\bar{\sigma}$, is of dominant importance. In pipe containing large flaw sizes, i.e. in section B, of fig. 8 the failure is dependent on the flaw size. In such a case the mode of failure is toughness dependent.

The recommended limit value for separating these two modes of pipe failure is that the normalized failure stress = 0.8, i.e.: M. $\sigma_c/\bar{\sigma} = 0.8$.

Substituting the appropriate values (σ_c =220 MPa, $\bar{\sigma}$ = 500 MPa), and using the

relation between M and the flaw length (eqn. 1 in the appendix), a critical length of ca 100 mm was obtained.

Thus for crack lengths $\lesssim$ 100 mm, the flow stress criterion

$$M.\ \sigma_c = \bar{\sigma} \quad \ldots \quad (5)$$

can be used with reasonable accuracy to predict failure stress level, σ_c . In fig.9 the solid line, curve I, was calculated from eqn. 3 in the appendix, the used M is 1.82, i.e. for failure mode A. Eqn. 4 in the appendix was used to generate the dashed curve II. Examining equations 3 & 4 indicates that curve II is the locus of points ($\sigma_c / \bar{\sigma}$) that have different M-values. Each point in curve II indicates the through flaw size corresponding to a definite failure stress, e.g. 272 MPa in case of M = 1.82. When a surface flaw becomes a through-wall flaw, continuous growth of this (initial) flaw will only take place if the stress is greater than the critical stress necessary to form the initial flaw. If the stress is less, no further enlargement will take place and leakage of the transmitted subjects through the pipe will continue.

In case of large surface cracks, 2c > 100 mm, the toughness dependent failure eqn. 2 was used to find the critical failure stress at 4 flaw lengths (2c): 100, 150, 200 and 300 mm, fig. 10a.

The same argument of the leakage or total rupture as above can also be made in this case, cf. fig 10b. In this fig. the failure stresses at different depths of these flaws were calculated by eqn. 3 in the appendix.

BS PD 6493:1980

The British standard published document BS PD 6493 is widely used in industry, e.g. [7, 8]. It is usually used in the assessment of the significance of weld defects. There are 11 failure modes covered by the PD 6493, and in our particular application, the susceptibility to fast brittle fracture will be considered. That is to say we are interested in the size and shape of flaws that may result in catastrophic failure, rather than the

time to obtain these defects.

An approach to evaluate the critical flaw sizes as recommended by PD 6493, is to evaluate a tolerable defect parameter $\bar{a}_m$ by using

$$\bar{a}_m = c\,(K_{Ic}/\sigma_y)^2 \quad \ldots \quad (6)$$

where c is given as a function of the applied stress in fig. 14 of that document. It is worth noting that $\bar{a}_m$ is half the critical defect size, i.e. there is an inherent safety factor in PD 6493.

The experimentally determined yield strength at the four different locations of our pipe, cf. fig. 1, were used in the above relation. The corresponding K_{Ic} at each location was taken as it had been estimated from the Charpy test.

The effective applied stresses are considered in two ways:

(a) Hoop stress caused by the internal pressure; 220 MPa.

(b) Hoop stress plus assumed residual stress from welding.

The PD6493 stipulates that the value to be used in calculation for any unknown residual stress is of the order of the parent metal yield stress. Thus a suitable value for this residual stress is 430 MPa, cf. fig. 1, and therefore the used stress for case (b) above is 650 MPa.

Table 3 shows the effective defect parameter, $\bar{a}_m$, at the shown pipe-locations assuming that the geometry of the surface cracks are highly affected by the circumferential normal stresses 220 and 650 MPa, ($\bar{a} = \bar{a}_m$). The effective defect parameter shown in the above table is then translated into real defect sizes and shapes using figure 12 of the PD 6493. The result for t/l = 0.1 is shown in table 4 where: e = material thickness, $\bar{a}$ = effective defect parameter, l = length of the defect and t = depth of the defect.

Some defect sizes and shapes that would initiate brittle failure are schematically drawn in fig. 11. In this fig. a selection of a through thickness defect ($2\bar{a}$ = e) and a surface defect for the ratio t/l = 0.1 was made at applied stress equal hoop stress, 220 MPa, fig. 11a and fig. 11b. The corresponding defect sizes in case of the present of the residual

stresses from welding, applied stress = 220 + 430 MPa, is also given in fig. 11c and fig. 11d.

CONCLUDING DISCUSSION

The difference between the measured mechanical properties at the base metal, HAZ and the weld were not found large except for the CVN fracture energy at and near the operating temperature of the pipe. Therefore it seems reasonable to suggest that a Charpy criterion should also be used for assessing the weld metal properties for the pipes intended to be used in our climate. Such a criterion should require the weld metal and the HAZ to meet the same minimum energy requirement as the parent metal.

Kiefner model predicts that failure in our pipe is leak-failure at such working stress of 220 MPa if a flaw of length 2C = 100 mm is present. This pipe will rupture if the stresses is raised to ca 272 MPa. The internal pressure in such a case is about 8.5 MPa ($\simeq$ 1234 Psi). The results can be seen together with the initial depths of the 100 mm surface cracks, in fig. 9. For cracks with lengths 2c > 100 mm, a toughness dependent failure equation should be used to predict the failure stress. Failure stresses for some flaw lengths and flaw depths are seen in fig. 10.

The failure criteria used in PD 6493 are fracture and plastic collapse. The fracture criterion is based on the COD-Design Curve, where stress or strain can be used for determining acceptable defect sizes, allowable loads and minimum toughness. The hoop stress which is expected from normal operating conditions, 220 MPa, and the total stresses assuming the presence of residual stress from welding, 650 MPa, were used. Fig. 11 summarizes some flaw dimensions that can cause failure in our pipe. For the considered ductile material, the PD 6493 required that the predicted tolerable depth of the surface flaw (a) is not large enough to induce plastic collapse. To check this it requires that the stress on the remaining ligament should not reach the flow stress. This is the case if the depth a $<$ e $(1 - \sigma \text{ applied} / \bar{\sigma})$

Using the appropriate values we conclude that for all a > 3.56 mm the failure in the pipe is induced by plastic collapse prior to failure by fracture.

The current analysis is incomplete in that we have not considered the failure of the pipe segment by the fatigue. While failure of the pipeline may be based on a critical defect size, it must also be recognized that the pipe line must operate under cyclic loads and thus are subject to failure by fatigue, [9].

In spite of the limitations in our analysis the predicted depths of the critical axial flaws are in good agreement with the available data on the thicknesses of a fractured segment from the above described pipe line, [10]. The documented thickness profiles of the fractured edges ere 70" length, and the thickness measurements were conducted at intervals of 0.5". For each fractured edge three different profiles were measured at 1/16", 1" and 2" from the edge. Fluctuations in thickness with a wave lengths ca 5" were observed in all profiles. The nearer the profile to the edge the lower its level and the larger are the amplitudes of each thickness-wave. The minimum thickness of ca 2 mm was measured, i.e. with corresponding thinning of ca 4.35 mm.

ACKNOWLEDGEMENTS

The materials were kindly put to our disposal by Kuwait Oil Company. The metallographic work was done at Kuwait Institute for Scientific Research. The authors wish to express their appreciation to Prof. B. Broberg and Prof. B. Bodelined of the Division of Solid Mechanics at Lund University, Sweden, for permission to use the test facilities. We also wish to thank the College of Technological Studies, PAAET, for providing facilities and assistance needed in the present work.

REFERENCES

1. J.F. Kiefner et al, ASTM STP 536,. 1973.
2. British Standard PD 6493: (1980) "Guidance on some methods for the derivation of acceptance levels for defects in fusion welded joints".
3. E. Kreyszig, Advanced Engineering Mathematics, 4th ed., John Wiley & Sons, 1979.
4. W.A. Maxey et al, The Fifth National Symposium on Fracture Mechanics, University of Illinois, 1971.
5. R.P. Reed et al, Welding Research Council Bulletin 245, 1979.
6. J.F. Kiefner et al, "Recent Research on Flaw Behavior During Hydrostatic Testing", American Gas Association Operating Section Transmission Conference, 1971.
7. J.D. Harrison, Fracture & Fracture Mechanics Case Studies, Edited by R.B. Tait et al, Pergamon Press, 1985.
8. R.B. Tait et al, ibid.
9. Y.F. Al-Obaid, et al, to be published.
10. Private Communications from Kuwait Oil Petroleum Company.

C	Si	Mn	P	S	Cr	Mo	Ti	Nb
0.08	0.20	1.10	0.018	0.002	0.03	0.01	0.018	0.039

Table 1: The chemical composition as given by the steel manufacturer.

	Original Area mm^2	Yield Strength MPa	Ultimate T.S., MPa	Fracture Strength MPa	Relative strain at Fracture
Base metal	44.15±0.23	437 ± 27	606 ± 3	412 ± 3	1
Weld + HAZ	42.77±1.20	430 ± 17	578 ± 10	441 ± 0.7	0.75

Table 2: The relevant tensile properties of small specimens of weld + HAZ only, and "equivelant" base metal.

Location as in fig.1	$\bar{a}$ (mm) values tabulated			
	Applied Stress A = 220 MPa	B = 650 MPa	Average for case A	B
1	10	1.99	9.8	2
2	9.6	2.1		
3	50.2	10.3	49.8	10.2
4	49.2	10.1		

Table: 3. The effective defect parameter, $\bar{a}$, at different pipe-locations based on the measured yield strength at these locations.

Location	Appl. Str. MPa.	$\bar{a}$ (mm)	$\bar{a}$/e	t/e values tabulated					
				t/1 = 0	0.1	0.2	0.3	0.4	0.5
1,2	220	9.8	1.54	0.37	0.63	0.97	-	-	-
3,4	220	49.8	7.84	0.54	-	-	-	-	-
1,2	650	2	0.31	0.18	0.24	0.30	0.37	0.46	0.54
3,4	650	10.2	1.61	0.38	0.65	0.91	-	-	-

Table: 4. Relative defect depths (t/e) for the effective defect parameters at the weld metal (locations 1 and 2) and at the base metal (locations 3 and 4) resulted from 220 and 650 MPa stresses.

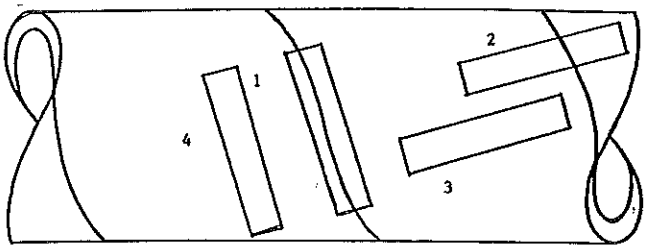

Fig.1
Location of the examined specimens with respect to the spiral weld-lines. Specimens 1 and 4 are in the rolling direction of the sheet-metal before fabrication. The following yield strength is the mean of 3 tests at each location. The drawing is not to scale.

Specimen	Yield Strength
2	472 MPa
1	456 "
3	433 "
4	430 "

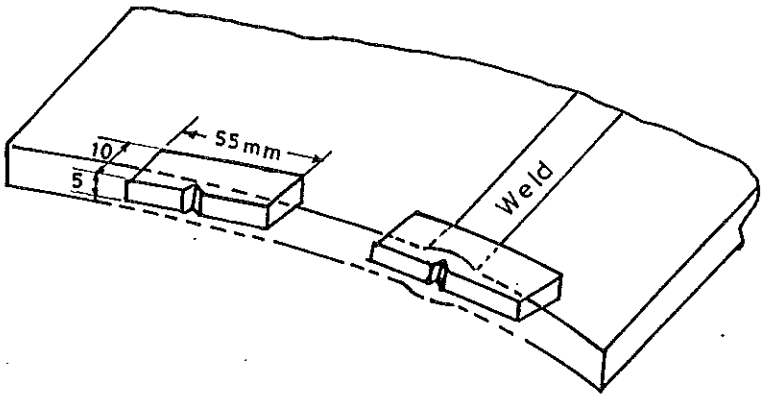

Fig.2
Sketch indicating the relative positions of two CVN specimens.

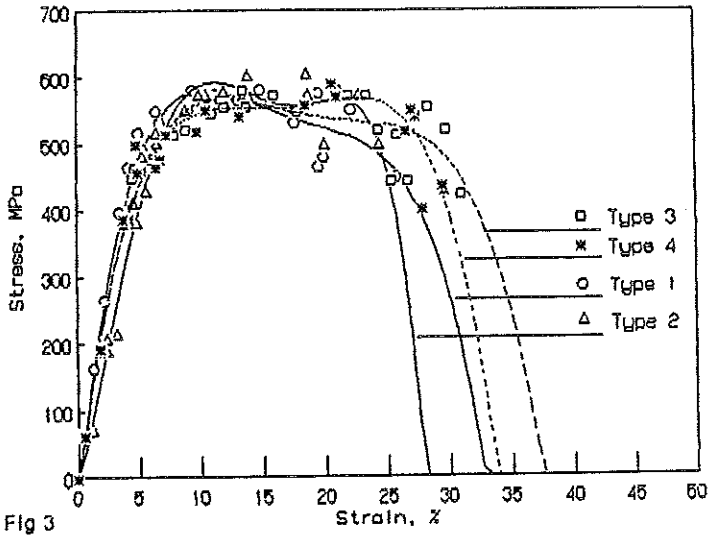

Fig 3

Fig.3
The tensile stress-strain curves for the four-specimen types. Each curve is the average of three individual runs. Note that the shown strain is calculated as the elongation measured by the cross-head movement of the tensile machine divided by a gauge length of 60 mm.

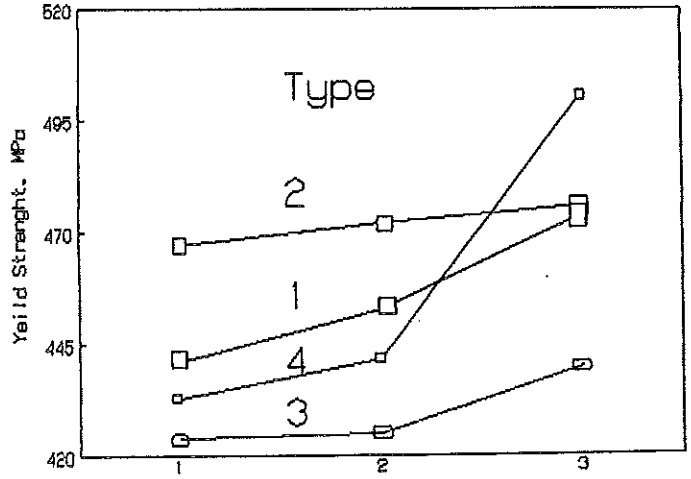

Fig 4 a

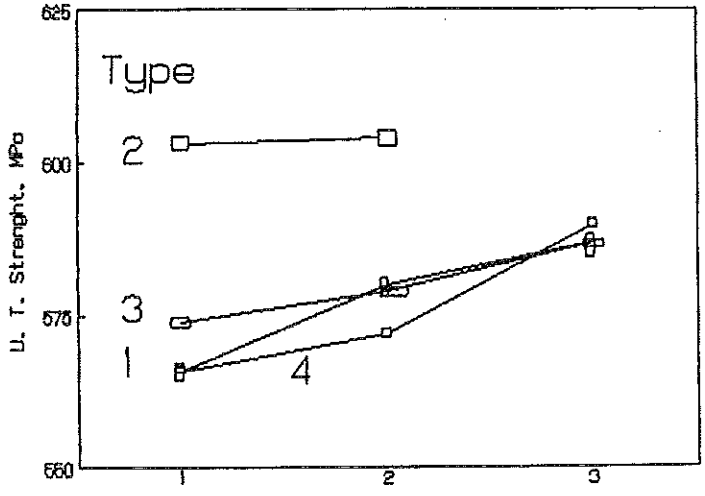

Fig 4 b

Fig.4
The individual values of the yield strength (4a) and ultimate strength (4b) measured at 12 different locations of the pipe. All tests were ended by rupture, except one test.

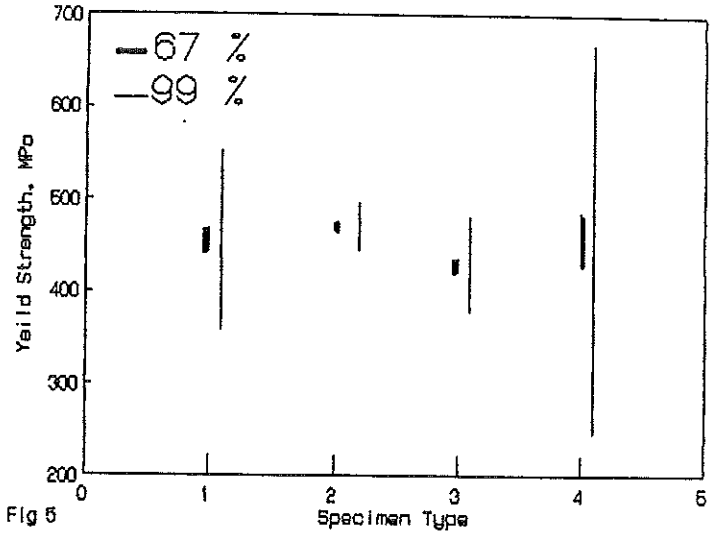

Fig.5
The 67% and 99% confidence degrees in the yield strength mean of each specimen type.

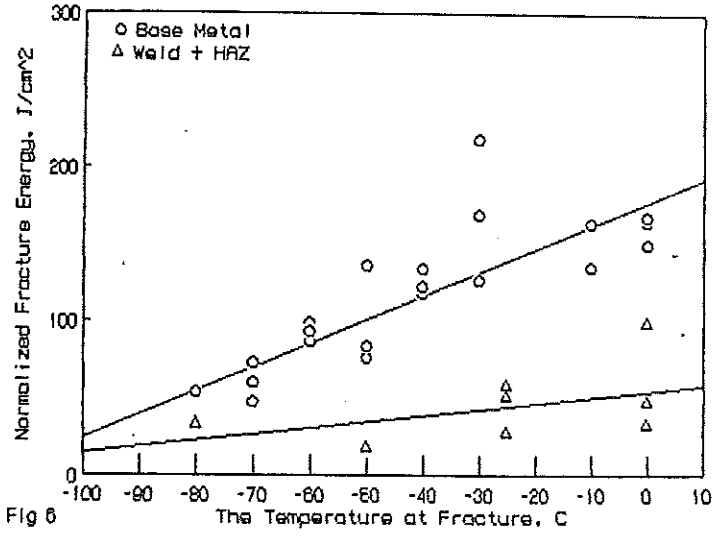

Fig.6
Raw data of Charpy tests at different temperatures. The measured fracture energy is normalized with respect to the actual fracture area under the notch.

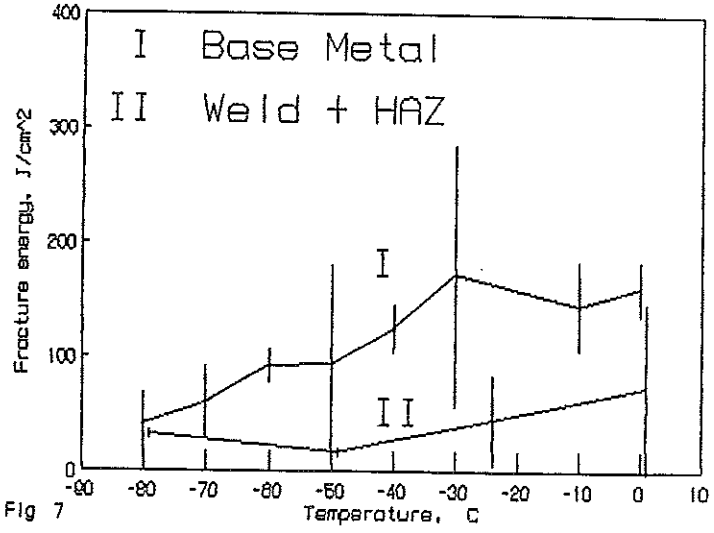

Fig.7
The mean and the limits to 95% confidence degree of the three-individual results of normalized Charpy Vee-notch fracture energy at each investigated temperature.

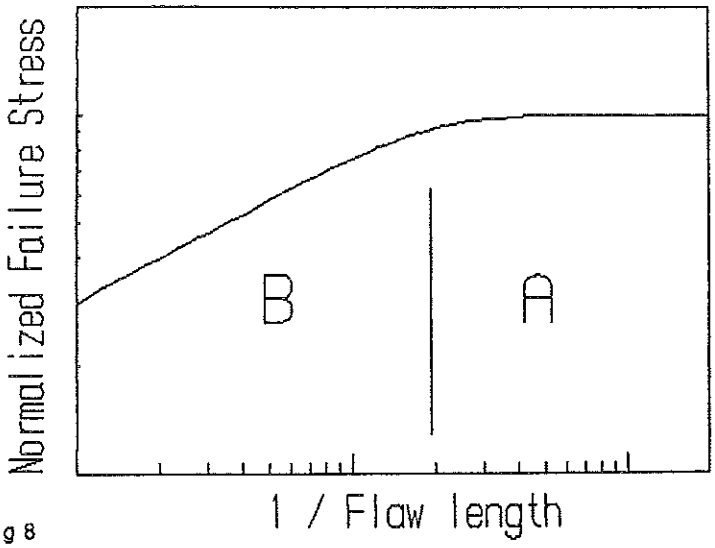

Fig 8

Fig.8
Pressurized pipe failure modes A and B according to flaw size and failure stresses: A = flow stress dependent failure, B = toughness dependent failure.

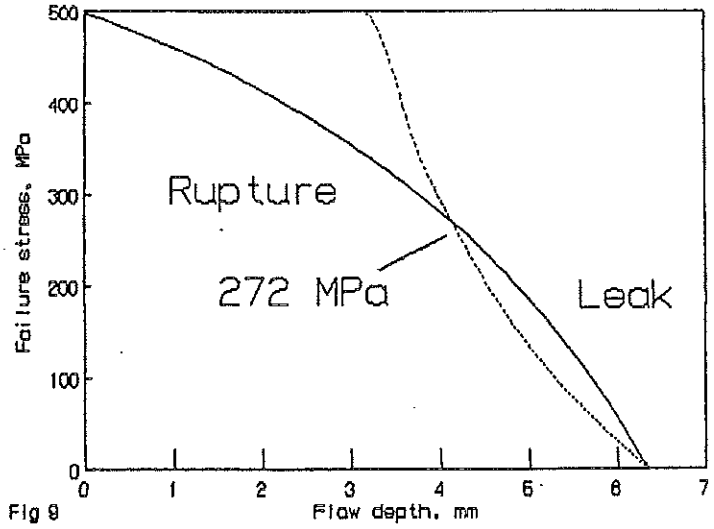

Fig 9

Fig.9
Failure stresses for the critical surface crack of length 100 mm with different depths. The conditions for leak and rupture modes of this crack are also shown.

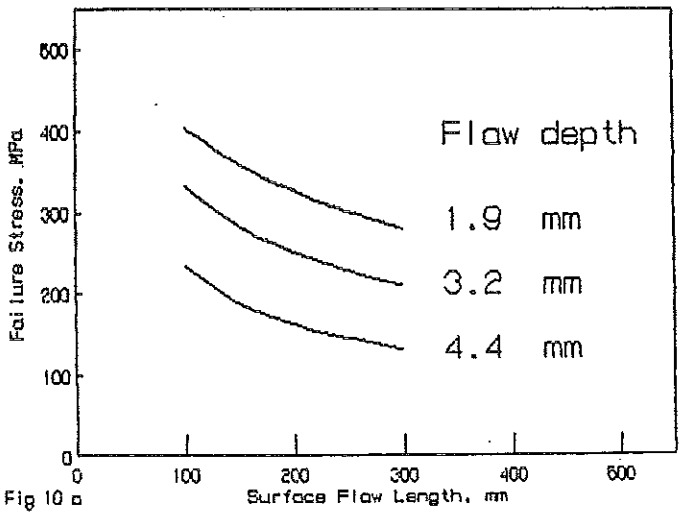

Fig 10 a

Fig.10a.
Failure stresses at large surface flaw lengths, for the 16" pipe as given the toughness dependent failure-mode.

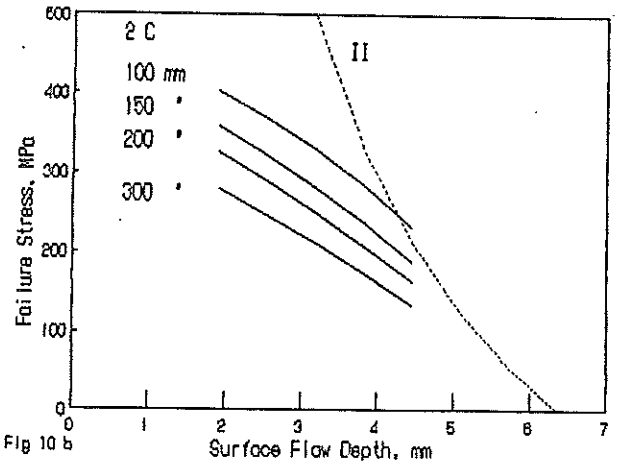

Fig.10b
Failure stresses for 100, 150, 200 and 300 mm surface crack lengths, at the shown depths. The leak or rupture failure type for each point is determined by its relative position to curve II.
Right = leak; Lift = rupture.

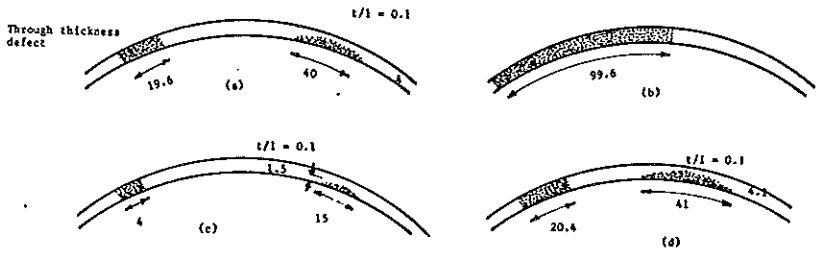

Fig.11
Collection of defect sizes and shapes that would initiate failure at and near the weld metal (a,c,d) or at the base metal (b). For case (a) and (b) an applied stress of 220 MPa is assumed. Additional residual stresses from welding ($= \sigma_y$) is assumed for cases (c) and (d). Shown dimensions are in mm.

APPENDIX

$$M \simeq \left[1 + 1.255 \frac{c^2}{Rt} - 0.0135 \frac{c^4}{R^2 t^2} \right]^{1/2} \quad \ldots (1)$$

$$\frac{K_c^2 \cdot \pi}{8c \cdot \bar{\sigma}^2} = \ln \sec \frac{\pi}{2} \frac{M \cdot \sigma_c}{\bar{\sigma}} \quad \ldots (2)$$

$$\sigma_c = \bar{\sigma} \cdot \frac{[1 - (d/t)]}{[1 - \frac{(d/t)}{M}]} \quad \ldots (3)$$

$$\sigma_c = \bar{\sigma} \cdot \frac{[1 - (d/t)]}{[1 - (\frac{d}{t})(\sigma_c / \bar{\sigma})]} \quad \ldots (4)$$

where:

M = Folias correction for pressurized pipe with axial flaws

$2c$ = Flaw length

R = Pipe radius

t = Pipe thickness

σ_c = Failure stress

$\bar{\sigma}$ = Flow stress

d = Flaw depth

K_c = Material property called plane stress fracture toughness

K_{Ic} = Plane strain fracture toughness